Polystyrene nanoplastics affect seed germination, cell biology and physiology of rice seedlings in-short term treatments: evidence of their internalization and translocation.

Carmelina Spanò[ab1], Simonetta Muccifora[c1], Monica Ruffini Castiglione[ab*], Lorenza Bellani[c], Stefania Bottega[a], Lucia Giorgetti[d]

[a] Department of Biology, University of Pisa, Via Ghini 13, 56126 Pisa, Italy
[b] Centre for Climate Change Impact, University of Pisa, 56124 Pisa, Italy
[c] Department of Life Sciences, University of Siena, Via A. Moro 2, 53100 Siena, Italy
[d] Institute of Agricultural Biology and Biotechnology, National Research Council, Via Moruzzi 1, 56124 Pisa, Italy

[1] co-first authors
*corresponding author
e-mail: monica.ruffini.castiglione@unipi.it

ABSTRACT

Agroecosystems represent more and more a huge long-term sink for plastic compounds which inevitably undergo fragmentation, generating micro- and nano-plastics, with potential adverse effects on soil chemistry and living organisms. The present work was focused on the short-term effects of two different concentrations of polystyrene nanoplastics (PSNPs) (0.1 or 1 g L^{-1} suspensions) on rice seedlings starting from seed germination, hypothesizing that possible acute effects on seedlings could depend on oxidative damage trigged by PSNPs internalization. As shown by TEM analysis, PSNPs were absorbed by roots and translocated to the shoots, affected root cell ultrastructure, the germination process, seedling growth and root mitotic activity, inducing cytogenetic aberration. Treatments were not correlated with increase in oxidative stress markers, but rather with a different pattern of their localization both in roots and in shoots, impairing H_2O_2 homeostasis and membrane damage, despite the adequate antioxidant response recorded. The harmful effects of PSNPs on cell

biology and physiology of rice seedlings could be caused not only by a direct action by the PSNPs but also by changes in the production / diffusion of ROS at the tissue / cellular level.

Keywords: antioxidant response; *Oryza sativa*; oxidative stress markers; polystyrene nanoplastics; toxicity; ultrastrucural analysis

1. Introduction

The use of plastics in many industrial fields and in everyday life has been affirmed since the '50s. Afterwards, plastic global production had an exponential increase from 2 million tons in 1950 up to around 370 million tons in 2019 (Plastics, 2020), with an uncontrolled and likely irreversible dumping into water systems, land, and air. Plastics persist in the environment and can undergo fragmentation into smaller pieces to generate fragments of various dimensions, up to microplastics (< 5 mm, MPs), and nanoplastics (< 100 nm in one dimension, NPs), the smaller fractions being of specific concern (Van Cauwenberghe et al., 2015; Blettler et al., 2017).

Micro and nano sized particles cannot be efficiently removed from the environment, and due to their small dimensions, can be directly ingested/inhaled or taken up by aquatic and terrestrial organisms, thus entering the food chain (Lwanga et al., 2016; Song et al., 2019).

Most studies reported plastic contamination in marine and fresh waters, but their presence in soils has only recently begun to be considered (Liu et al., 2018). It has been estimated that the terrestrial environment can represent a greater long-term sink for MPs and NPs accumulation than the marine environment, by at least a factor of four (Horton et al., 2017). Contamination of farming soils can have various origins, including amendment practices with fertilizers and biosolid, plastic mulching, irrigation, swamping, littering and deposition from the atmosphere (Bläsing and Amelung, 2018), with adverse effects on soil chemistry and living organisms. Once in farmlands, as mentioned above, plastics undergo ageing and breakup in MPs and in NPs, the latter being difficult to quantify for the

complexity of the matrix (Hurley and Nizzetto, 2018). Although in the last three years works have been published on these subjects, the understanding of the risks connected with the interactions between MPs and NPs with crops is still very scarce. Surprisingly, a greater number of reviews and generalist articles are published at the moment, rather than experimental works on this issue. However, the results achieved so far evidenced the ability of MP/NP to enter the plants (Mateos-Cardenas et al., 2021, and references therein) with a consequent potential hazard for animal, human and environmental health.

Though NPs, able to permeate bio-membranes (Bouwmeester et al., 2015; EFSA, 2016; Nel et al., 2009), are potentially more hazardous than MPs, very few studies have analysed the effects of these particles on plants.

Oxidative stress, morphotoxicity, and cytogenotoxicity induced by polystyrene nanoplastics (PSNPs) were reported in *Allium cepa* (Maity et al., 2020). In the same plant system, the recorded cellular and physiological injuries were associated with both mechanical action of PSNPs on the root surface, and with their internalization in different cellular compartments (Giorgetti et al., 2020).

Conflicting results were found by Lian et al. (2020) in wheat, in which PSNPs did not disturb seed germination, but rather increased root elongation, biomass, C and N content, and partially reduced the accumulation of some micronutrients. Furtherly, metabolic analysis revealed that PSNPs positively modulated energy production and aminoacid metabolism (Lian et al., 2020).

In the wake of the increasing attention given to the potential toxicity of NPs for plants, our focus was on rice, *Oriza sativa* L. which is a very important cereal for human nutrition, providing food to more than half of the global population (Zhou et al., 2021). Based on the common agricultural techniques, rice can be germinated in flooded fields, or in dry soils which undergo flooding after rice germination. For this procedure, usually river water is used as irrigation source. This implies that during germination, rice can be exposed to micro and nanoplastics *via* the aquatic medium and *via* the sediments of the soils (Larue et al., 2021). In previous research on rice, the effects of long-term treatment with 20 nm PSNPs, their transport of PSNPs from culture medium to roots with a negative

effect on the seedling development and a modulation of the expression of disease resistance functional genes have been recorded after 16 days of treatment (Zhou et al., 2021). Our interest was instead on the early stages of the growth of rice seedlings focusing on the short-term effects/uptake of PSNPs, short-term treatments being particularly effective towards different toxicants for cyto-genotoxicity evaluations in terms of root meristem analysis and oxidative stress.

The hypothesis was that possible acute effects on seedlings could rely on oxidative injury trigged by PSNPs internalization. To develop this working hypothesis some complementary technical approaches have been applied to get a clear picture of the effects of the treatments imposed on the plant under study. Germination, roots and shoots growth, genotoxicity, oxidative stress and antioxidant response, and submicroscopical effects were considered, after an exposure to an environmentally relevant concentration (Giorgetti et al., 2020) of 0.1 g L^{-1}, compared to a relatively high concentration of 1 g L^{-1} of PSNPs, to better evaluate the possible acute toxicity of PSNPs in short-term tests.

2. Materials and Methods

2.1. Polystyrene nanoplastics and plant material

Polystyrene microspheres (PSNPs), Visiblex TM Color Dyed Microspheres (nominal size 50 nm), were purchased by Phosphorex, Inc. (South St. Hopkinton, MA01748).

Grains of *Oryza sativa* L., var. Cerere (kindly provided by SA.PI.SE Coop. Agr., Vercelli, Italy), after visual selection, were surface sterilised for 15 min in 5% sodium hypochlorite and rinsed before use. Grains were germinated in the dark at 25 ± 1 °C in Petri dishes (30 grains x 10 dishes for control and each treatment) with water (control) or with a 0.1 or 1 g L^{-1} suspension of PSNPs. At 96 h, germination percentage was recorded, and the length of roots and shoots measured. In addition, vigour index (V. I.) was also calculated with the following formula:

V. I. = Germination (%) x Seedling Growth (mm).

After measurements, seedlings were collected, vigorously washed with deionized water and roots and shoots were isolated and used fresh, stored at -80°C (for biochemical determinations) or fixed as specified below.

2.2. TEM observations

To observe the isolated polystyrene microspheres, a drop (10 µl) of the PSNPs 1 g L-1 suspension was placed on TEM grids covered with formvar, allowed to settle and to dry (Giorgetti et al., 2020). Small cubes of control and treated roots and shoots were pre-fixed in Karnovsky solution (Karnovsky, 1965), post-fixed in osmium tetroxide, dehydrated and embedded in Epon 812-Araldite A/M mixture. Thin sections were stained with uranyl acetate and lead citrate. Isolated PSNPs and root and shoot sections were observed under a FEI Tecnai G2 Spirit electron microscope at 100 kV.

2.3. Cytogenetic studies

Ten roots for control and each treatment were fixed overnight in ethanol/glacial acetic acid (3:1 v/v) and then stained following Feulgen stain procedure (Giorgetti et al., 2011). For cytological analysis, 1000 nuclei were randomly analysed by light microscope from each slide with five replicates for each treatment. Since the rice chromosomes are very small, to have a better resolution, Feulgen-stained root meristems were also observed under fluorescence microscope at 560 nm, wavelength specific for pararosaniline (Böhm and Sprenger, 1968).

Mitotic activity was expressed as mitotic index (MI, number of mitosis per 100 nuclei) to estimate the levels of cytotoxicity of the treatments. Mitotic aberrations (number of aberrations per 100 nuclei) were determined for the genotoxicity analysis of the treatments. The cytological aberrations observed in dividing cells included chromosomal bridges and fragments, lagging chromosomes, c metaphases and disturbed anaphases.

2.4. Histochemical detection of hydrogen peroxide and lipid peroxidation

Five roots and five shoots of comparable size and length for each treatment were sectioned with hand microtome in the area of root maturation and above the coleoptile node, respectively. Slices of control samples were stained with toluidine blue for a conventional anatomical evaluation. Amplex Ultrared

133 probe (Life Technologies, USA) was applied for *in situ* detection of hydrogen peroxide (H_2O_2) as
134 previously described (Spanò et al., 2020). Red fluorescence (568ex/681em nm) developed was
135 proportional to the amount of hydrogen peroxide in the sample. The free radical sensor BODIPY1
136 581/591C11 (Life Technologies, USA), applied at the concentration of 10 mM in PBS 0.1 M pH 7.4,
137 allowed to evaluate lipid peroxidation (Giorgetti et al., 2019). After acquiring simultaneously the
138 green (485ex/510em nm) and the red fluorescence (581ex/591em nm) signals, the two images were
139 merged and analysed. Optical microscope analysis was performed with a Leitz Diaplan, equipped
140 with a Leica DCF420 ccd camera. Fluorescence microscope analysis was carried out with a Leica
141 DMLB, equipped with appropriate set of excitation/emission filters and with a Leica DC300 ccd
142 camera.
143 *2.5. Determination of hydrogen peroxide and thiobarbituric acid reactive substances (TBARS)*
144 Hydrogen peroxide content of roots and shoots was determined according to Jana and Choudhuri
145 (1982). After extraction with phosphate buffer 50 mM pH 6, the homogenate was centrifuged at
146 6,000g for 25 min. and mixed with 0.1% titanium chloride in 20% (v/v) H_2SO_4. The mixture was then
147 centrifuged at 6000g for 15 min and the absorbance of supernatant was read at 410 nm. The
148 concentration of H_2O_2 was calculated from a standard curve and expressed as μmol g^{-1}FW. Lipid
149 peroxidation was estimated in terms of TBARS according to Wang et al. (2013) with minor
150 modifications as in Spanò et al. (2017). The concentration of TBARS was expressed as nmol g^{-1}FW,
151 measuring the specific absorbance at 532 nm and subtracting the non-specific absorbance at 600 nm.
152 Calculation was made basing on an extinction coefficient of 155 mM^{-1} cm^{-1}.
153 *2.6. Enzyme extraction and assays*
154 Antioxidant enzymes were extracted as in Spanò et al. (2013). After grounding in liquid nitrogen with
155 a mortar and pestle (4 °C), roots and shoots were homogenised in 100 mM potassium phosphate
156 buffer (pH 7.5) containing 1 mM ethylenediaminetetraacetic acid (EDTA), and 30%
157 polyvinylpyrrolidone (PVP-40). The homogenate was centrifuged at 15,000g for 20 min and
158 supernatants were collected and stored at − 80 °C until use for enzymatic assays. Ascorbate

peroxidase (APX, EC 1.11.1.11) activity was measured according to Nakano and Asada (1981) by the decrease in absorbance at 290 nm (extinction coefficient 2.8 mM^{-1} cm^{-1}) as ascorbate was oxidized. Correction for the low, non-enzymatic oxidation of ascorbate by hydrogen peroxide (blank) was made. Catalase (CAT, EC 1.11.1.6) activity was determined as described by Aebi (1984) and calculated using the 39.4 mM^{-1} cm^{-1} extinction coefficient. A blank containing only the enzymatic solution was made. Superoxide dismutase (SOD, EC 1.15.1.1) activity was determined as in Beyer and Fridovich (1987) with minor modification as in Spanò and Bottega (2016). One SOD unit was defined as the amount required to inhibit by 50% the photoreduction of nitroblue tetrazolium, determined spectrophotometrically at 550 nm. Guaiacol peroxidase (POX, EC 1.11.1.7) activity was determined as described by Arezki et al. (2001). 1% guaiacol was used as substrate and the activity was measured determining guaiacol oxidation by H_2O_2 at 470 nm (extinction coefficient 26.6 mM^{-1} cm^{-1}), one unit oxidizing 1.0 μmol guaiacol per min. All enzymatic activities were determined at 25 °C and expressed as U mg^{-1} protein. Protein measurement was performed according to Bradford (1976), using BSA as standard.

2.7. Electrophoretic peroxidase separation

Electrophoresis was performed on 10% PAGE as in Milone et al. (2003) with minor modifications as in Sorce et al. (2017), using Tris-HCl 1.5 M pH 8.8. Equal amounts (25 μg) of proteins extracted from roots and shoots were loaded onto electrophoretic gel. After running (200 V, constant current of 35 mA gel^{-1}), bands were visualized by incubation in the dark for 90 min in 1 M Na-acetate buffer pH 4.6 containing 0.04% benzidine and 10 mM H_2O_2. Enzyme activity appeared as dark brown bands.

2.8 Statistical analysis

Data were expressed as mean of at least four replicates ± SE. Before analysis, normality of distribution and homogeneity of variances were verified. The results were processed by one-way analysis of variance (ANOVA) followed by *post hoc* multiple comparisons (Tukey test). The level of significance was $p < 0.05$.

3. Results and Discussion

3.1. PSNPs are taken up by roots, inducing ultrastructural alterations, and translocated to shoots.

Isolated PSNPs showed irregular shapes and diameters ranging from 20 to about 200 nm, 85% having at least one axis minor than 100 nm (Fig. 1a) (Giorgetti et al., 2020). In root cells, under both PSNPs treatments, nanoplastics were detectable in cytoplasm and vacuoles as single particles, or in the form of more or less numerous aggregates, mainly localized in the cells of the cortical parenchyma (Fig. 1b and 1c) and in some xylem vessels (Fig.1d). Rare PSNPs, mostly isolated, were detected in shoot. Figure 1e shows a representative image in which PSNPs were present in coleoptile cells. The cortical cells under all treatments appeared in slight plasmolysis and showed ultrastructural alterations in the mitochondrial crests and in the reticulum membranes (Fig. 1f). Some electron dense bodies were observed in the space between the wall and the plasmalemma (Fig. 1f). Shoot cells showed no significant ultrastructural alterations (data not shown). To the best of our knowledge, only few papers have demonstrated that NPs can be taken up by crop plants and translocated from root to shoot (Lian et al., 2020; Giorgetti et al., 2020; Sun et al., 2020; Zhou et al., 2021). As in *A. cepa* (Giorgetti et al., 2020), electron microscopy allowed to perform a fine analysis at ultrastructural level, showing the presence of PSNPs in different cellular compartments and demonstrating the ability of rice to absorb PSNPs in the very early stages of development. Evidence of PSNPs root absorption and translocation to the aboveground tissue were also evidenced in rice plants after long term exposure to PS at nano and at microscale by confocal microscope observations (Liu et al., 2022).

Other studies reported that MP/NP uptake by plants may depend both on the size and shape of the materials, on the aggregation tendency and ability to alter the pore diameter of the cell wall, influencing the dynamic behaviour of its components (Maity and Pramanick, 2020), which in turn can be modulated in response to environmental stressors (Chialva et al., 2019). These reflections may sustain the results published by Conti et al. (2020), the only research, at present, proving the presence of MP and NP in vegetables and fruits purchased from local markets. In this regard, however, it was not demonstrated by which route these plastics would reach the edible tissues of the plant.

3.2. PSNPs affect the whole germination process, seedling growth and root apical meristem behaviour, without altering the general anatomy of the seedling.

The minimum germination percentage was recorded under 0.1 g L^{-1} treatment with a value significantly lower than 1 g L^{-1} treatment. Neither of the treatments were significantly different from the control (Table 1). Our results are in partial discordance with previous studies on *A. cepa* and wheat (Giorgetti et al., 2020; Lian et al., 2020) where no significant influence of PSNPs on germination was observed. As in *A. cepa* (Giorgetti et al., 2020), in rice there was a gradual significant decrease in root length at increasing PSNPs concentration, while a significant decrease in shoot length was recorded only under 1 g L^{-1} treatment (Table 1). Roots seemed therefore to be more sensitive than shoots to PSNPs, probably for their direct contact with the suspension and for their function of uptake (Rillig et al., 2019; Zhou et al., 2020). Further information derived from V. I. (Table 1), that, combining both germination and growth parameters, can give a more exhaustive picture of seedling establishment. According to Lian et al. (2020), V. I. parameter may be particularly useful, given the high germinability of our seed batch (over 90%). Based on the above, the gradual decrease in V. I. with increasing PSNPs concentration, clearly showed an impairment of the whole germination process.

Cytogenetic analysis in root meristems of *O. sativa* (chromosome number 2n = 24) evaluated the MI, the percentage of mitotic phases and the percentage of abnormal mitoses induced by the treatments. Due to the small size of the rice chromosomes, no micronuclei, derived from chromosomal breaks, was observed and, consequently, it was not possible to highlight the genotoxicity effect with micronucleus test. Mitotic index analysis in control and PSNPs treated roots (Figure 2a) indicated significant inhibitory effects on mitotic activity only at the highest concentration of 1 g L^{-1} PSNPs, corresponding to a decrease of 34.85% of mitotic activity in respect to the control. This result differed from that previously observed in *A. cepa* (Giorgetti et al., 2020) in which the inhibitory effect on MI was observed also at the dose of 0.1 g L^{-1}, suggesting that the extent of cytotoxic response may depend on the considered plant species.

Analysis of mitotic phases frequencies was reported in Table 2. Interestingly, both treatments with PSNPs induced substantial changes in the percentages of the various phases. Higher percentages of total metaphases (> 32%) and anaphases/telophases (37 to 42%) were detected in PSNPs-treated meristems compared to control (about 26 and 25% respectively). This was due to the significant increase of C metaphase and anaphase anomalies and could result from a blockage or slowing of the mitotic cycle, probably related to mitotic spindle failure or disturbance. The cytological anomalies, especially c- metaphases, increased in 1 g L^{-1} PSNPs treatment, although the differences between 1 and 0.1 g L^{-1} were not statistically significant. This result agreed with our previous work (Giorgetti et al., 2020) highlighting that cytological aberrations could arise even at low doses, without significant increase at the highest concentrations.

The percentage of total abnormal mitosis are showed in Figure 2b. Treatments with 0.1 and 1 g L^{-1} PSNPs induced 35.77% and 40.83% of cytological anomalies, respectively, while in control abnormal mitoses were rarely observed.

C metaphases (Figure 3a, b) represented one of the most common anomalies at metaphases, but also lagging (Figure 3c, d) and sticky chromosomes (Figure 3h, i) were observed in both PSNPs treatments; cytological anomalies at anaphase/telophase mainly consisted in chromosome lagging and bridges (Figure 3j-l).

As reported above, these abnormal cytological events could result by mitotic spindle defects or by clastogenic effects, the latter inducing breakage, stickiness or reunion of chromosome, directly or indirectly determined by the PSNPs exposure. Previous studies on plant and animal cells (Gopinath et al., 2019; Matthews et al., 2021) indicated that genotoxicity was likely induced by oxidative stress and ROS production rather than by direct action of PSNPs at DNA and mitotic spindle level. On the other hand, chromatin injuries oxidative stress-independent cannot be ruled out.

Even if it was not possible to evaluate the genotoxic damage with the micronucleus test, the results of cytogenetic analysis indicated at least the involvement of the mitotic spindle in generating cytological anomalies leading to polyploidy and aneuploidy as a consequence of c-metaphases and

chromosome laggings, followed by the incorrect distribution of sister chromatids in daughter cells. In addition, multipolar spindles and chromosome grouping were also observed (Figure 3e-g) and these anomalies might further trigger genetic alteration towards haploid condition and chromosome size reduction. The high frequency of cytological anomalies found in rice may also be related to an intrinsic chromosomal instability due to the polyploid origin of the rice genome (Levy and Feldman, 2002). The large presence of repetitive sequences, retroelements, transposons, could further increase the susceptibility of rice genome producing chromosomal rearrangements in response to the environmental stress, in this case to the stress induced by PSNPs treatments starting from the first stages of imbibition (Fan et al., 2008; Jiang et al., 2003).

To well characterise the plant system from an anatomical point of view, histological analysis of roots and shoots was also performed, without showing substantial differences depending on the treatments. Root cross sections were done in the area of maturation allowing to distinguish, from outside to inside, rhizodermis, exodermis, sclerenchyma, cortical parenchyma and endodermis. The central cylinder was organized in a pericycle delimiting the hexarch stele (Figure 4Aa).

Figure 4Ba shows a representative shoot cross section taken above the coleoptile node. The coleoptile was evident as the outermost portion of the section surrounding two young leaves. In the coleoptile an external and internal epidermis enfolded the mesophyll, in which two vascular bundles were located facing each other in a symmetrical way. At the small depression in the external epidermis the split area was recognizable, in which the coleoptile was divided becoming a sheath. Below, rolled foliage leaves (Primary and Second leaf) were recognizable, the first of which showing a hint of aerenchymatous cavities.

3.3. PSNPs treatments were not associated with increase in oxidative stress markers, but with a different pattern of their localization.

Recent data have shown that PSNPs, likewise metal nanoparticles, can induce oxidative stress in plants (Giorgetti et al., 2020; Ruffini Castiglione et al., 2014). It is known that, to counteract this

287 stress, plants can activate an antioxidant response in which low molecular weight molecules cooperate
288 with antioxidant enzymes to control ROS concentration and oxidative damage.
289 In our experimental conditions, neither in roots or in shoots there was an increase in hydrogen
290 peroxide content with increasing PSNPs concentration (Table 3). Under 0.1 g L^{-1} PSNPs treatment,
291 the concentration of this ROS was even significantly lower in comparison with control and under 1 g
292 L^{-1} PSNPs (Table 3). TBARS concentration significantly decreased in treated roots at increasing
293 PSNPs concentration (Table 3a), all these results suggesting the involvement of an adequate
294 antioxidant response to counteract ROS damage. The effects of nanoplastics on oxidative *status* seem
295 to depend on plant species, as different results were recorded in onion roots (Giorgetti et al., 2020)
296 treated with PSNPs of comparable size: in fact, in *A. cepa* under 1 g L^{-1} PSNPs both hydrogen
297 peroxide and TBARS reached the highest concentration.
298 Given these quantitative results, the impaired chromatin behaviour observed by cytogenetic analysis
299 could seem not related to oxidative stress, but the different localization pattern of oxidative stress
300 markers described below could have an impact. However, other mechanisms, ROS-independent,
301 leading to genomic DNA disturbances could not be ruled out.
302 Histochemical tests in root cross sections for *in situ* detection of H_2O_2 (Fig. 4Ab-d) showed tissues
303 differently responsive to staining procedure: in both control and treatments rhizodermis, exodermis,
304 and sclerenchyma were strongly positive to Amplex probe, as well as the central cylinder. In the
305 stele, particularly deep staining was detectable for xylem vessels. Under 1 g L^{-1} PSNPs the red signal
306 was more widespread, also involving cortex. Despite the of H_2O_2 detected biochemically, the spread
307 of the signal to all root tissues, particularly to the cortex, at the highest concentration treatment, may
308 represent an impairment in H_2O_2 homeostasis/diffusion and/or a way to trigger specific responses
309 related to root development. A similar response has been recorded in *A. cepa* roots treated with 1 g
310 L^{-1} of 50 nm PSNPs, that involved, in addition to root epidermis and vascular tissues, also the cortex
311 (Giorgetti et al., 2020). The application of Amplex probe to shoot cross sections (Fig. 4Bb-d) allowed
312 to appraise a faint signal on the coleoptile and its two vascular bundles, and a deeper staining at the

313 level of the first leaf, in control and in 0.1 g L^{-1} treated samples. Under 1g L^{-1} treatment the red signal
314 also extended to the second leaf showing a different pattern of hydrogen peroxide presence, also
315 involving the younger leaf.
316 Root lipid peroxidation pattern, as revealed by Bodipy probe, (Fig. 4Ae-g) was clearly
317 superimposable to that of hydrogen peroxide in control samples. In all samples the green signal was
318 diffused mainly in the exodermis and sclerenchyma portion (in particular for 1 g L^{-1}), but more intense
319 in the central cylinder for 0.1 g L^{-1} and in the cortex for 1 g L^{-1}. In the shoot a good correspondence
320 between Amplex and Bodipy staining (Fig. 4Be-g) was also highlighted; the only difference involved
321 the external epidermis of the coleoptile, which, in all treatments, was strongly positive for the Bodipy
322 staining, while it was not for Amplex probe. Also in this case, the treatments were able to alter the
323 localization pattern of the probe, indicating the direct effects of the PSNPs on the integrity of the
324 membranes, belonging to different tissues and organs. As demonstrated for metal nanoparticles
325 (Muccifora et al., 2021) local production of ROS, would lead to the degradation of structures such as
326 cell membrane and cell wall, allowing possible PSNPs entrance and movement. These data were
327 supported by the observations at the TEM (Fig. 1) which attested the internalization of PSNPs of
328 different sizes, even up to 200 nm, their presence in the cells of the root, in the vessels and even if
329 rare in the shoot. Furthermore, the alterations of the ultrastructure observed in treatments, were overall
330 in the membranes of mitochondria and endoplasmic reticulum.
331 *3.4. Rice under PSNPs treatments displayed an adequate antioxidant response to face oxidative*
332 *injuries*
333 Regarding antioxidant response, the focus was on main hydrogen peroxide scavenging enzymes. In
334 particular, APX can scavenge H_2O_2 using ascorbate as reducing agent, while CAT is able to directly
335 scavenge it catalysing a dismutation reaction (Mhamdi et al., 2010). A significant increase in APX
336 activity was detected under 1 g L^{-1} both in roots and in shoots (Table 3), in accordance with what
337 previously observed in *Cucumis sativus* leaves treated with 100 nm PSNPs (Li et al., 2020), suggesting
338 a role for APX in H_2O_2 scavenging under PSNPs treatment. CAT activity (Table 3) reached the

maximum value under 1 g L^{-1} in shoots (Table 3b) while in roots (Table 3a) there were not significant differences among the different treatments. Both PSNPs-concentration-dependent decrease (Li et al., 2020) and increase (Zhou et al., 2021) in CAT activity are reported in literature. From the present work an organ-dependent pattern can be suggested. SOD can directly modulate the levels of H_2O_2 carrying out the dismutation of superoxide radicals into molecular oxygen and H_2O_2. For these reasons, SOD is considered a primary defence against different stress conditions (Tyagi et al., 2019). In accordance with previous studies on rice (Zhou et al., 2021), a gradual increase in SOD activity was recorded in roots (Table 3a) with significant difference, however, only between control and 1 gL^{-1}. In shoots (Table 3b) SOD activity showed the minimum value under 0.1 g L^{-1}. Guaiacol peroxidases (class III peroxidases) can participate in several processes in plants, being able to act through a peroxidative and/or a hydroxylic cycle (Passardi et al., 2005). In the peroxidative cycle, POX can reduce hydrogen peroxide catalysing the oxidation of various substrates, such as phenolics and lignin precursors (Cosio and Dunand, 2009), assisting in this way APX and CAT in hydrogen peroxide scavenging. Guaiacol peroxidases are involved in a wide range of physiological processes including cell wall metabolism, lignification and suberization, auxin catabolism and stress response (Pandey et al., 2017). Both in roots and in shoots the maximum value of soluble POX activity was found in 1 gL^{-1} treatment (Table 3). However, while in shoots (Table 3b) there was a gradual increase of this enzyme activity, in roots (Table 3a) there was a significant decrease, under 0.1 g L^{-1} treatment in comparison with control seedlings. The patterns of POX activity (Fig. 5), evidenced by in-gel activity assay, differed in roots (Fig. 5a) and shoots (Fig. 5b): a band with lower mobility (1) was visible only in roots, while shoots were characterized by the presence of two bands (4, 5) with higher mobility, gradually increasing with PSNPs concentration. Other bands (2, 3) were present both in roots and in shoots, band 3 reaching the highest intensity at the highest PSNPs concentration. Changes induced by PSNPs on both the activity and the electrophoretic pattern of POX are consistent with the effects of these materials on growth and in accordance with the widely accepted role of peroxidases in lignin polymerization.

4. CONCLUSIONS

The results of the present work have clearly shown that PSNPs can be absorbed and moved to the above ground part of rice seedlings already at the first stages of plant development. The presence of PSNPs was associated with ultrastructural alterations, limited to root cells, inhibition of mitotic activity and impairment of the germination process and seedling growth. These last disturbances were also consistent with the activity/pattern of guaiacol peroxidases, widely accepted as important factors in the regulation of growth and development. The compromised chromatin behaviour observed by cytogenetic analysis and the ultrastructure damages seemed not necessarily related to oxidative stress that perhaps, thanks to an adequate antioxidant response (APX, POX), was not increased under PSNPs treatments. Despite the lack of oxidative stress markers increase, however, histochemistry allowed to record different patterns in the localization of both hydrogen peroxide and membrane damage, highlighting that PSNPs could impair homeostasis/diffusion of H_2O_2 and cause localized membrane damage in plants as also evidenced by TEM analysis. These damages could be induced not only by changes in the production / diffusion of ROS at the tissue and cellular level, but also by a direct action by the PSNPs, taken up and translocated by the plant.

Acknowledgments: Authors acknowledge SA.PI.SE Coop. Agr.,Vercelli, Italy for having kindly provided grains *Oryza sativa*, var. Cerere. This work was financed by local funding of the University of Pisa (ex 60%) and supported by University of Siena and National Research Council of Italy.

391 **References**

392

393 Aebi, H., 1984. Catalase *in vitro.* Methods Enzymol. 105, 121-126.

394 Arezki, O., Boxus, P., Kevrs, C., Gaspar, T., 2001. Changes in peroxidase activity and level compounds
395 during light-induced plantlet regeneration from *Eucalyptus camaldulensis* Dehn. nodes *in vitro*. Plant
396 Growth Regul. 33, 215-219.

397 Beyer Jr, W.F., Fridovich, I., 1987. Assaying for superoxide dismutase activity: some large
398 consequences of minor changes in conditions. 161, 559-566.

399 Bläsing, M., Amelung, W., 2018. Plastics in soil: analytical methods and possible sources. Sci. Total
400 Environ. 612, 422-435.

401 Blettler, M.C.M., Ulla, M.A., Rabuffetti, A.P., Garello, N., 2017. Plastic pollution in freshwater
402 ecosystems: macro-, meso-, and microplastic debris in a floodplain lake. Environ. Monit. Assess. 189,
403 581.

404 Böhm, N., Sprenger, E., 1968. Fluorescence cytophotometry: A valuable method for the quantitative
405 determination of nuclear Feulgen-DNA. Histochemie 16, 100-118.

406 Bouwmeester, H., Hollman, P.C.H., Peters, R.J.B., 2015. Potential health impact of environmentally
407 released micro- and nanoplastics in the human food production chain: experiences from
408 nanotoxicology. Environ. Sci. Technol. 49, 8932-8947.

409 Bradford, M., 1976. A rapid and sensitive method for the quantitation of microgram quantities of
410 protein utilizing the principle of protein-dye binding. Anal. Biochem. 72, 248-254.

411 Chialva, M., Fangel, J.U., Novero, M., Zouari, I., Salvioli di Fossalunga, A., Willats, W.G.T.,
412 Bonfante, P., Balestrini, R., 2019. Understanding changes in tomato cell walls in roots and fruits: the
413 contribution of arbuscular mycorrhizal colonization. Int. J. Mol. Sci. 20, 415.

414 Conti, G.O., Ferrante, M., Banni, M., Favara, C., Nicolosi, I., Cristaldi, A., Fiore, M., Zuccarello, P.,
415 2020. Micro- and nano-plastics in edible fruit and vegetables. The first diet risks assessment for the
416 general population. Environ. Res. 187, 109677.

417 Cosio, C., Dunand, C., 2009. Specific functions of individual class III peroxidase genes. J. Exp. Bot.
418 60, 391-408.
419 EFSA Panel on Contaminants in the Food Chain (Contam), 2016. Presence of microplastics and
420 nanoplastics in food, with particular focus on seafood. 14, 4501. doi: 10.2903/j.efsa.2016.4501
421 Fan C., Zhang Y., Yu Y., Rounsley S., Long M., Wing R.A., 2008. The Subtelomere
422 of *Oryza sativa* Chromosome 3 Short Arm as a Hot Bed of New Gene
423 Origination in Rice. Mol. Plant 1, 839-850. https://doi.org/10.1093/mp/ssn050.
424 Giorgetti, L., Ruffini Castiglione, M., Turrini, A., Nuti Ronchi, V., Geri, C., 2011. Cytogenetic and
425 histological approach for early detection of "mantled" somaclonal variants of oil palm regenerated
426 by somatic embryogenesis: first results on the characterization of regeneration system. Caryologia
427 64, 223-234.
428 Giorgetti, L., Spanò, C., Muccifora, S., Bellani, L., Tassi, E., Bottega, S., Di Gregorio, S., Siracusa,
429 G., Sanità di Toppi, L., Ruffini Castiglione, M., 2019. An integrated approach to highlight biological
430 responses of *Pisum sativum* root to nano-TiO_2 exposure in a biosolid-amended agricultural soil. Sci.
431 Total Environ. 650, 2705-2716.
432 Giorgetti, L., Spanò, C., Muccifora, S., Bottega, S., Barbieri, F., Bellani, L., Ruffini Castiglione, M.,
433 2020. Exploring the interaction between polystyrene nanoplastics and *Allium cepa* during
434 germination: Internalization in root cells, induction of toxicity and oxidative stress. Plant Physiol.
435 Biochem. 149: 170-177.
436 Gopinath, P.M., Saranya, V., Vijayakumar, S., Meera, M.M., Ruprekha, S., Kunal, R., Pranay, A.,
437 Thomas, J., Mukherjee, A., Chandrasekaran, N., 2019. Assessment on interactive prospectives of
438 nanoplastics with plasma proteins and the toxicological impacts of virgin, coronated and
439 environmentally released-nanoplastics. Sci. Rep., 9, 8860.
440 Horton, A.A., Walton, A., Spurgeon, D.J., Lahive, E., Svendsen, C., 2017. Microplastics in freshwater
441 and terrestrial environments: evaluating the current understanding to identify the knowledge gaps and
442 future research priorities. Sci. Total Environ. 586, 127-141.

443 Hurley, R.R., Nizzetto, L., 2018. Fate and occurrence of micro(nano)plastics in soils: knowledge gaps
444 and possible risks. Curr. Opin. Environ. Sci. Health, 1, 6-11.
445 Jana, S., Choudhuri, M.A., 1982. Glycolate metabolism of three submerged aquatic angiosperms
446 during aging. Aquat. Bot. 12, 345-354.
447 Jiang, N., Bao, Z., Zhang, X., Eddy, S. R., McCouch, S R., Wessler, S. R., 2003. An active DNA
448 transposon family in rice. Nature 421, 163–167. https://doi.org/10.1038/nature01214
449 Karnovsky, M.J., 1965. A formaldehyde-glutaraldehyde fixative of high osmolality for use in electron
450 microscopy. J. Cell Biol. 27, 137-138.
451 Larue, C., Sarret, G., Castillo-Michel, H., Pradas del Real, A.E., 2021. A critical review on the impacts
452 of nanoplastics and microplastics on aquatic and terrestrial photosynthetic organisms. Small 17,
453 2005834
454 Levy, A.A., Feldman, M., 2002. The impact of polyploidy on grass genome evolution Plant Physiol.
455 130, 1587-1593.
456 Li, Z., Li, R., Li, Q., Zhou, J., Wang, G., 2020. Physiological response of cucumber (*Cucumis sativus*
457 L.) leaves to polystyrene nanoplastics pollution. Chemosphere 255, 127041.
458 Lian, J., Wu, J., Xiong, H., Zeb, A., Yang, T., Su, X., Su, L., Liu, W., 2020. Impact of polystyrene
459 nanoplastics (PSNPs) on seed germination and seedling growth of wheat (*Triticum aestivum* L.). J.
460 Hazard. Mater. 385, 121620.
461 Liu Y., Guo R., Zhang S., Sun, Y., Wang, F., 2022. Uptake and translocation of nano/microplastics by
462 rice seedlings: Evidence from a hydroponic experiment. J. Hazard. Mater. 421, 126700.
463 Liu, M., Lu, S., Song, Y., Lei, L., Hu, J., Lv, W., Zhou, W., Cao, C., Shi, H., Yang, X., He, D., 2018.
464 Microplastic and mesoplastic pollution in farmland soils in suburbs of Shanghai, China. Environ.
465 Pollut. 242, 855-862.
466 Lwanga, E.H., Gertsen, H., Gooren, H., Peters, P., Salánki, T., van der Ploeg, M., Besseling, E.,
467 Koelmans, A.A., Geissen, V., 2016. Microplastics in the terrestrial ecosystem: implications for
468 *Lumbricus terrestris* (Oligochaeta, Lumbricidae). Environ. Sci. Technol. 50, 2685-2691.

Mateos-Cárdenas, A., van Pelt, F.N.A.M., O'Halloran, J., Jansen, M.A.K., 2021. Adsorption, uptake and toxicity of micro- and nanoplastics: effects on terrestrial plants and aquatic macrophytes. Environ. Pollut. 284, 117183.

Maity, S., Chatterjee, A., Guchhait, R., De, S., Pramanick, K., 2020. Cytogenotoxic potential of a hazardous material, polystyrene microparticles on *Allium cepa* L. J. Hazard. Mater. 385, 121560.

Maity, S., Pramanick, K., 2020. Perspectives and challenges of micro/nanoplastics-induced toxicity with special reference to phytotoxicity. Glob. Chang. Biol. 26, 3241-3250.

Matthews, S., Mai, L., Jeong, C.B., Lee, J.S., Zeng, E.Y., Xu, E.G., 2021. Key mechanisms of micro- and nanoplastic (MNP) toxicity across taxonomic groups. Comp. Biochem. Physiol. C Toxicol. Pharmacol. 247, 109056.

Mhamdi A., Queval G., Chaouch S., Vanderauwera S., Van Breusegem F., Noctor G., 2010. Catalase function in plants: A focus on *Arabidopsis* mutants as stress-mimic models. J. Exp. Bot. 61, 4197-4220.

Milone, M.T., Sgherri, C., Clijsters, H., Navari-Izzo, F., 2003. Antioxidative responses of wheat treated with realistic concentration of cadmium. Environ. Exp. Bot. 50, 265-276.

Muccifora, S., Castillo-Michel, H., Barbieri, F., Bellani, L., Ruffini Castiglione, M., Spanò, C., Pradas del Real, A.E., Giorgetti, L., Tassi, E.L., 2021**.** Synchrotron radiation spectroscopy and transmission electron microscopy techniques to evaluate TiO_2 NPs incorporation, speciation, and impact on root cells ultrastructure of *Pisum sativum* L. plants. Nanomaterials 11, 921.

Nakano, Y., Asada, K., 1981. Hydrogen peroxide is scavenged by ascorbate-specific peroxidase in spinach chloroplasts. Plant Cell Physiol. 22, 867-880.

Nel, A.E., Mädler, L., Velegol, D., Xia, T., Hoek, E.M.V., Somasundaran, P., Klaessig, F., Castranova, V., Thompson, M., 2009. Understanding biophysicochemical interactions at the nano-bio interface. Nat. Mater. 8, 543-557.

Pandey, V.P., Awasthi, M., Singh, S., Tiwari, S., Dwivedi, U.N., 2017. A Comprehensive review on function and application of plant peroxidases. Biochem. Anal. Biochem. 6, 1000308.

Passardi, F., Cosio, C., Penel, C., Dunand, C., 2005. Peroxidases have more functions than a Swiss army knife. Plant Cell Rep. 24, 255-265.

Plastics – the Facts, 2020 – PlasticsEurope https://www.plasticseurope.org

Rillig, M.C., Lehmann, A:, deSouza Machado, A.A., Yang, G., 2019. Microplastic effects on plants. New Phytol. 223, 1066-1070.

Ruffini Castiglione, M., Giorgetti, L., Cremonini, R., Bottega, S., Spanò, C., 2014. Impact of TiO_2 nanoparticles on *Vicia narbonensis* L.: potential toxicity effects. Protoplasma 251, 1471-1479.

Song, Y., Cao, C., Qiu, R., Hu, J., Liu, M., Lu, S., Shi, H., Raley-Susman, K.M., He, D., 2019. Uptake and adverse effects of polyethylene terephthalate microplastics fibers on terrestrial snails (*Achatina fulica*) after soil exposure. Environ. Pollut. 250, 447-455.

Sorce, C., Montanaro, G., Bottega, S., Spanò C., 2017. Indole-3-acetic acid metabolism and growth in young kiwifruit berry. Plant Growth Regul. 82, 505-515.

Spanò, C., Bottega, S., 2016. Durum wheat seedlings in saline conditions: salt spray versus root-zone salinity. Estuar. Coast. Shelf Sci. 169, 173-181.

Spanò, C., Bottega, S., Bellani, L., Muccifora, S., Sorce, C., Ruffini Castiglione, M., 2020. Effect of zinc priming on salt response of wheat seedlings: relieving or worsening? Plants 9, 1514.

Spanò, C., Bruno, M., Bottega, S., 2013. *Calystegia soldanella*: dune versus laboratory plants to highlight key adaptive physiological traits. Acta Physiol. Plant. 35, 1329-1336.

Spanò, C., Bottega, S., Ruffini Castiglione, M., Pedranzani, H.E., 2017. Antioxidant response to cold stress in two oil plants of the genus *Jatropha*. Plant Soil Environ. 63, 271-276.

Sun, X.D., Yuan, X.Z., Jia, Y., Feng, L.J., Xing, B., 2020. Differentially charged nanoplastics demonstrate distinct accumulation in *Arabidopsis thaliana*. Nat. Nanotechnol. 15, 755-760.

Tyagi, S., Shumayla, Singh, S.P., Upadhyay, S.K., 2019. Role of superoxide dismutases (SODs) in stress tolerance in plants, in: Singh, S., Upadhyay, S., Pandey, A., Kumar, S. (Eds.) Molecular approaches in plant biology and environmental challenges. energy, environment, and sustainability. Springer, Singapore.

559 Van Cauwenberghe, L., Devriese, L., Galgani, F., Robbens, J., Janssen, C.R., 2015. Microplastics in
560 sediments: a review of techniques, occurrence and effects. Mar. Environ. Res. 111, 5-17.
561 Wang, Y.S., Ding, M.D., Gu, X.G., Wang, J.L., Pang, Y.L., Gao, L.P., Xsia T., 2013. Analysis of
562 interfering substances in the measurement of malonildialdehyde content in plant leaves Am. J.
563 Biochem. Biotechnol. 9, 235-242.
564 Zhou, A., Zhang, Y., Xie, S., Chen, Y., Li, X., Wang, J., Zou, J., 2021. Microplastics and their potential
565 effects on the aquaculture systems: a critical review. Aquac. 13, 719-733.
566
567
568
569
570
571
572
573
574
575
576
577
578
579
580
581
582
583
584
585
586
587
588
589
590
591
592
593
594
595
596
597
598
599

Figure Captions

Figure 1.
TEM images of: a) an aggregate of PSNPs from 1 g L^{-1} suspension. (b-f) TEM images from *O. sativa* seedlings after 96 h of seed imbibition; b) PSNPs aggregate (arrow) in a portion of cytoplasm of 1 g L^{-1} treated root cell; c) PSNPs (arrow) in a vacuole of 0,1 g L^{-1} treated root cell; d) PSNPs (arrows) in a vessel of 1 g L^{-1} treated root; e) PSNPs (arrow) in a vacuole of 1 g L^{-1} treated shoot cell; f) portion of cytoplasm of 1 g L^{-1} treated root: electrondense bodies in the space between wall and plasmalemma (arrows), portions of endoplasmic reticulum (arrow heads). M, mitochondrion; V, vacuole; W wall.

Figure 2.
Effect of PSNPs (0.1 and 1 g L^{-1}) on mitotic index (a) and on cytological anomalies (b) in *O. sativa* root apical meristem after 96 h of seed imbibition. The reported data are expressed as mean values ± standard error. Different letters indicate significant differences by post hoc Tukey text ($p \leq 0.05$).

Figure 3.
Examples of cytological anomalies in *O. sativa* root meristems analyzed after 96 h of seed imbibition in water (control) and in the presence of 0.1 g L^{-1} (a, c, e, g, i, k) and 1 g L^{-1} (b, d, f, h, j, l) nano PS; a) polyploidy c metaphase, b-d) c metaphases, e-g) abnormal metaphases with chromosome grouping, h, i) abnormal anaphases with sticky and lagging chromosomes, j, k) chromosome bridges at anaphase, l) chromosome bridge in a possibly haploid anaphase. bar = 5 µm.

Figure 4.
A. Cross hand sections of *O. sativa* roots of seedlings after 96 h of imbibition in water (control), and in the presence of PSNPs. The plate comprehends representative images of root sections of control samples stained with (a) toluidine blue, (b) Amplex Ultrared probe for *in situ* detection of hydrogen peroxide, (e) BODIPY probe for *in situ* detection of TBARS. Representative root cross sections of samples treated with 0.1 and 1 gL^{-1} of PSNPs stained with AMPLEX probe and with BODIPY probe are reported in (c-d) and (f-g) respectively. rhi= rhizodermis, ex= exodermis, sc= sclerenchyma, co= cortex, e=endodermis, p=pericycle, st= stele.
B. Cross hand sections of *O. sativa* shoots of seedlings after 96 h of imbibition in water (control), and in the presence of PSNPs. The plate comprehends representative images of shoot sections of control samples stained with (a) toluidine blue, (b) Amplex Ultrared probe for *in situ* detection of hydrogen peroxide, (e) BODIPY probe for *in situ* detection of TBARS. Representative shoot cross sections of samples treated with 0.1 and 1 gL^{-1} of PSNPs stained with AMPLEX probe and with BODIPY probe are reported in (c-d) and (f-g) respectively. C= coleoptile, vb= vascular boundle, PL= primary leaf, SL= second leaf, ae= aerenchyma. Split=coleoptile splitting zone.

Figure 5.
Native PAGE gel of guaiacol peroxidase from roots (a) and shoots (b) of *O. sativa* seedlings after 96 h of seed imbibition in water (control, C) and in the presence of 0.1 g L^{-1} and 1 g L^{-1} PSNPs. Bands are indicated by arrows.

Table 1. Germination percentage and vigour index of grains, root and shoot length of seedlings of *O. sativa* after 96 h of imbibition in water (control) and in the presence of 0.1 g L^{-1} and 1 g L^{-1} PSNPs.

	C	0.1 gL^{-1} PSNPs	1 gL^{-1} PSNPs
Germination (%)	95.56±0.98 ab	93.78±0.93 b	97.12±0.91 a
Vigour Index	3568.38±81.24 a	3072.63±55.67 b	2361.50±50.43 c
Root length (mm)	27.40±0.84 a	23.10±0.81 b	15.93±0.61 c
Shoot length (mm)	9.94±0.29 a	9.66±0.32 a	8.39±0.41 b

The reported data represent mean values ± SE. Within row, values followed by different letters are statistically significant with Tukey test for $P \leq 0.05$

Table 2. Cytological analysis of mitotic phases in root meristem cells of *Oryza sativa* after 7 days of seed imbibition in water (control, C) and in the presence of 0.1 g L^{-1} and 1 g L^{-1} PSNPs.

	C	0.1 gL^{-1} PSNPs	1 gL^{-1} PSNPs
% Normal Prophases	48.36 ± 4.29a	29.3 ± 1.62b	25.18 ± 3.20b
% Normal Metaphases	22.50 ± 0.66a	12.93 ± 1.28b	6.91 ± 2.10b
% Abnormal Metaphases	3.81 ± 1.94b	20.49 ± 0.65a	25.29 ± 3.67a
% Normal Anaphase/ Telophases	24.77± 3.07a	22.01 ± 2.32a	27.08 ± 0.60a
% Abnormal Anaphase/ Telophases	0.56 ± 0.56b	15.27 ± 2.03a	15.54 ± 1.37a

Values are the means values 100 mitosis analysed in four replicates (n=4 ± SE). Within row, values followed by different letters are statistically significant with Tukey test for $P \leq 0.05$

Table 3. Concentration of hydrogen peroxide and thiobarbituric acid reactive substances (TBARS), and activity of guaiacol peroxidase (POX), ascorbate peroxidase (APX), catalase (CAT) and superoxide dismutase (SOD) in roots and shoots of *Oryza sativa* seedlings after 7 days of seed imbibition in water (control, C) and in the presence of 0.1 g L^{-1} and 1 g L^{-1} PSNPs.

Roots

	C	0.1 gL^{-1} PSNPs	1 gL^{-1} PSNPs
Hydrogen peroxide (µM g^{-1}FW)	0.61±0.04 a	0.30±0.07 b	0.50±0.06 a
TBARS (nanomol g^{-1}FW)	15.57±0.12 a	13.08±0.20 b	11.28±0.20 c
POX (U mg^{-1})	0.51±0.01 b	0.38±0.01 c	0.58±0.02 a
APX (U mg^{-1})	0.58±0.04 b	0.56±0.03 b	1.18±0.02 a
CAT (U mg^{-1})	2.04±0.17 a	1.67±0.18 a	1.90±0.30 a
SOD (U mg^{-1})	33.46±3.74 b	40.48±0.74 ab	43.08±0.97 a

Shoots

	C	0.1 gL^{-1} PSNPs	1 gL^{-1} PSNPs
Hydrogen peroxide (µM g^{-1}FW)	1.10±0.15 a	0.73±0.04 a	1.25±0.32 a
TBARS (nanomol g^{-1}FW)	10.12±0.15 a	9.61±0.20 b	9.97±0.08 ab
POX (U mg^{-1})	0.23±0.01 c	0.30±0.00 b	0.37±0.01 a
APX (U mg^{-1})	1.47±0.03 b	1.51±0.01 b	1.69±0.03 a
CAT (U mg^{-1})	2.75±0.17 b	2.17±0.08 b	3.86±0.32 a
SOD (U mg^{-1})	45.80±1.33 a	34.03±4.00 b	42.52±1.25 ab

Valuea are the means of six replicates ± SE. Within row, values followed by different letters are statistically significant with Tukey test for $P \leq 0.05$

673 Figure 1
674

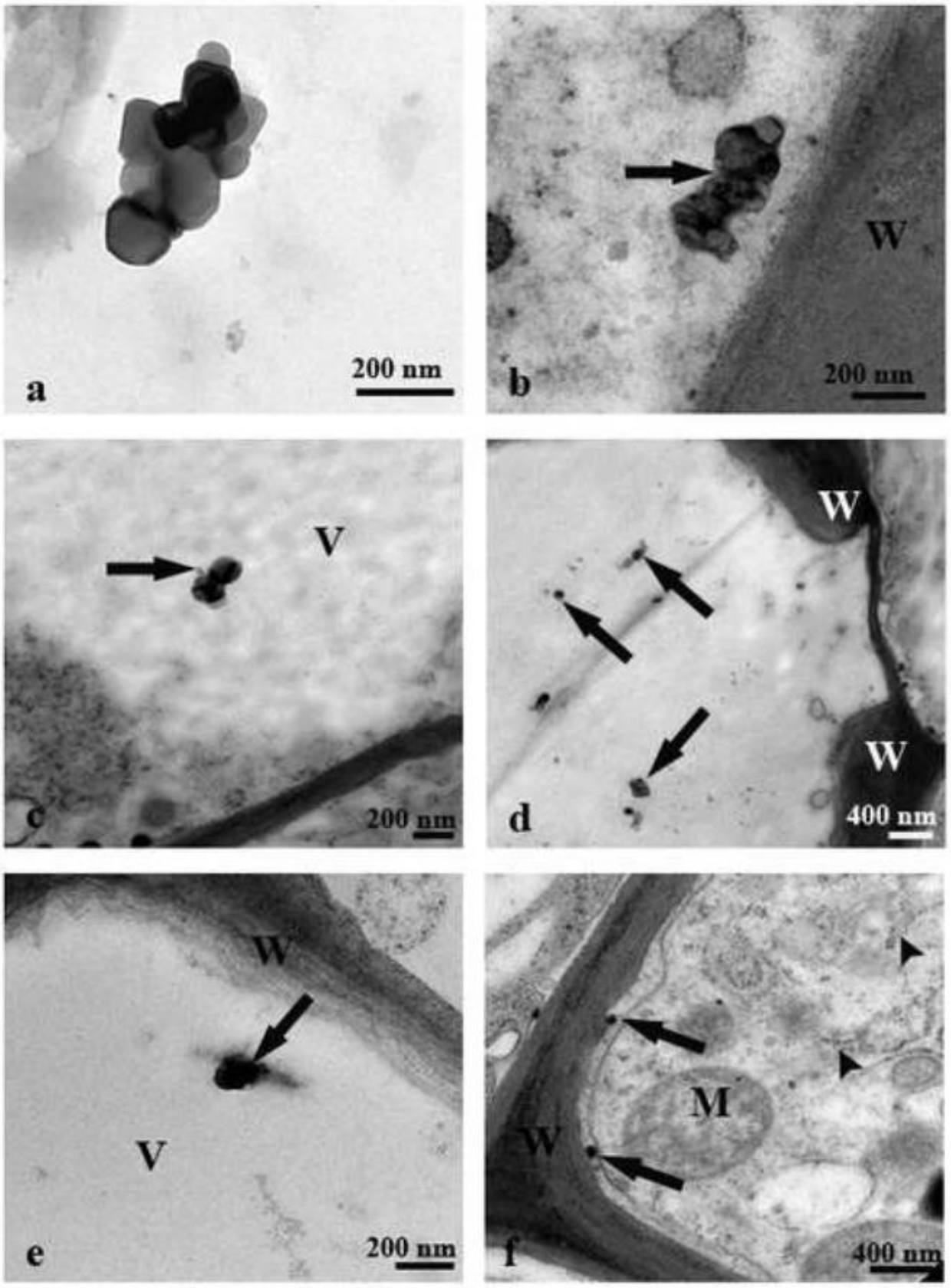

675
676

Figure 2

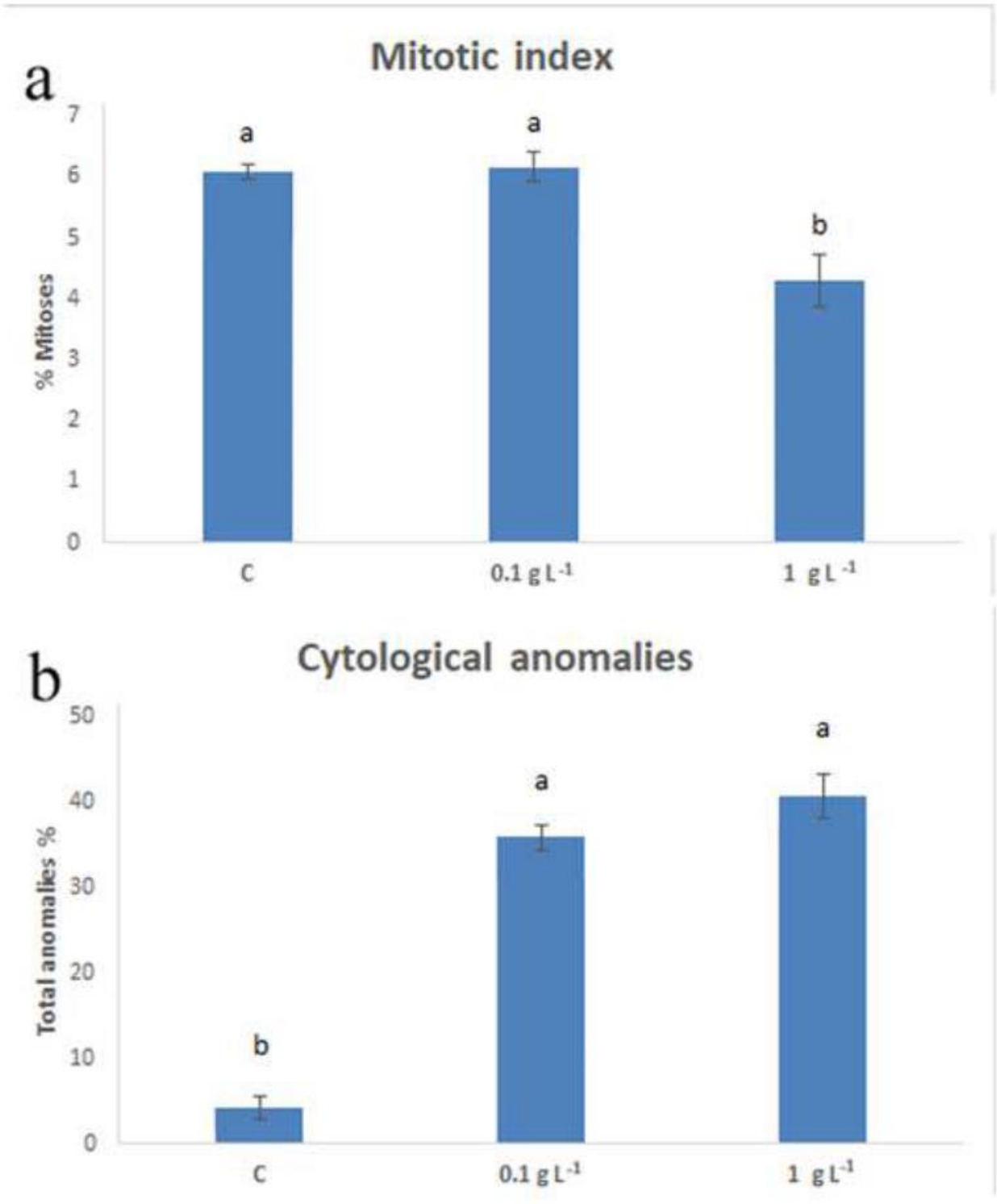
a
Mitotic index
% Mitoses
7
6
5
4
3
2
1
0
a
a
b
C
0.1 g L-1
1 g L-1
b
Cytological anomalies
Total anomalies %
50
40
30
20
10
0
b
a
a
C
0.1 g L-1
1 g L-1

Figure 3

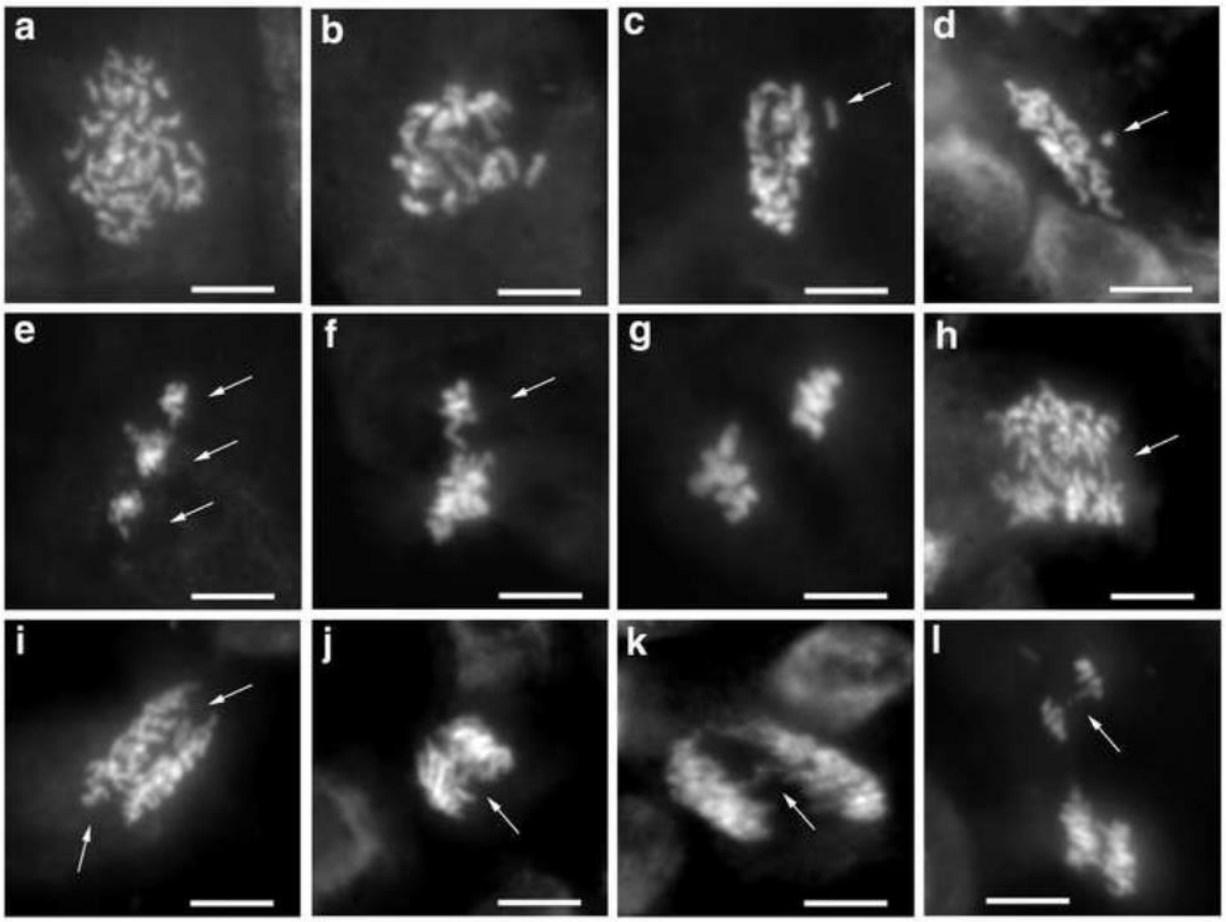

Figure 4

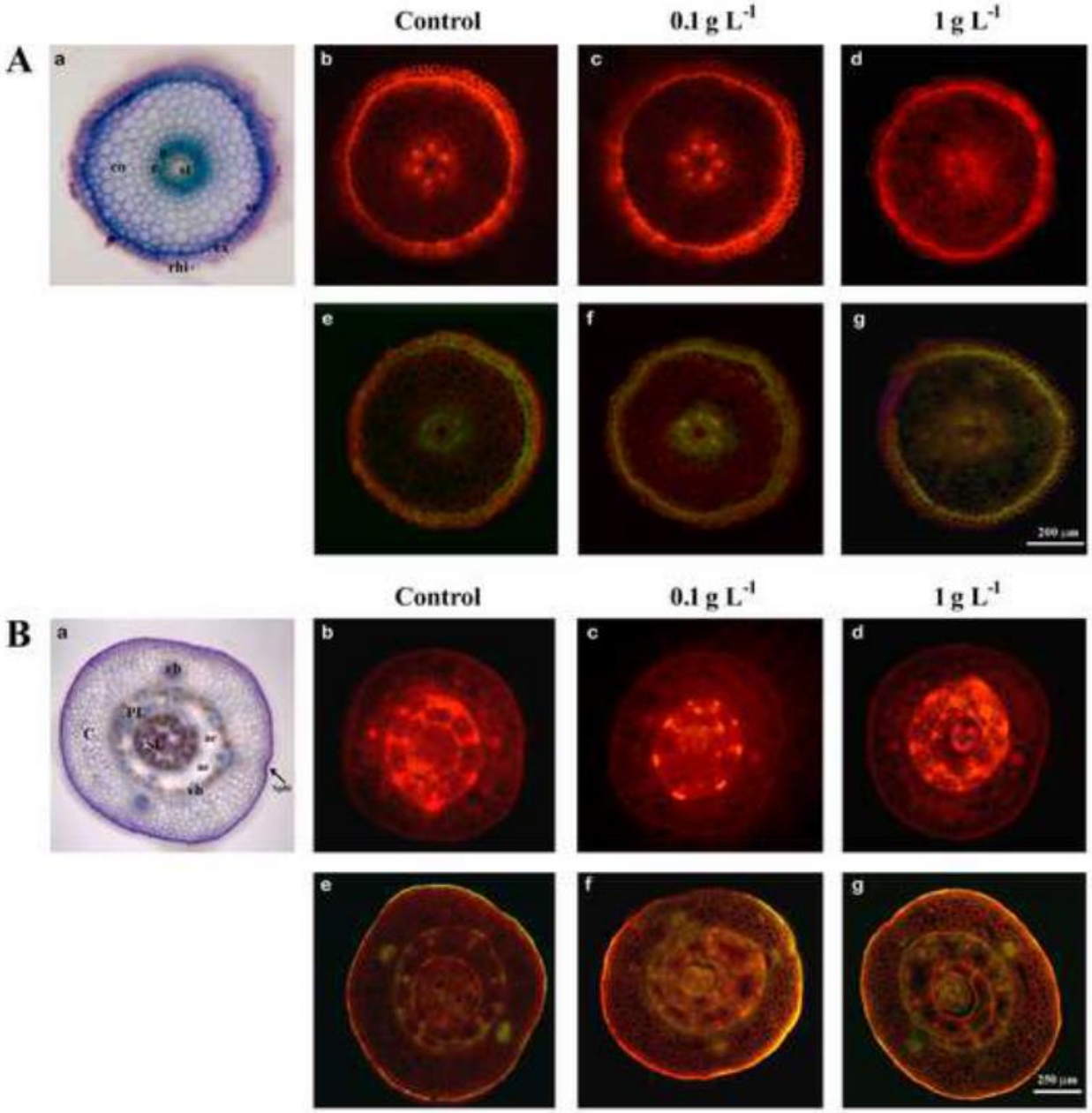
A
B
Control
0.1 g L-1
1 g L-1
a
b
c
d
e
f
g
co
ct
rhi
ex
ep
PE
C
vb
200 µm
250 µm

Figure 5